PHYSICAL REVIEW E **78**, 025203(R) (2008)

Nanostructures with long-range order in monolayer self-assembly

Feng Shi,[1] Pradeep Sharma,[1,2,*] Donald J. Kouri,[2,3] Fazle Hussain,[1,2] and Gemunu H. Gunaratne[2,4,†]

[1]*Department of Mechanical Engineering, University of Houston, Houston, Texas 77204, USA*

[2]*Department of Physics, University of Houston, Houston, Texas 77204, USA*

[3]*Department of Chemistry, University of Houston, Houston, Texas 77204, USA*

[4]*The Institute for Fundamental Studies, Kandy, Sri Lanka*

(Received 4 March 2008; revised manuscript received 10 July 2008; published 19 August 2008)

A key ingredient for continued expansion of nanotechnologies is the ability to create perfectly ordered arrays on a small scale with both site and size control. Self-assembly—i.e., the spontaneous formation of nanostructures—is a highly promising alternative to traditional fabrication methods. However, efforts to obtain perfect long-range order via self-assembly have been frustrated in practice as ensuing patterns contain defects. We use an idea based on the fundamental physics of pattern formation to introduce a strategy to consistently obtain perfect patterns.

DOI: 10.1103/PhysRevE.78.025203 PACS number(s): 89.75.Kd, 61.46.Hk

Most innovative applications of nanoscience, such as memory devices, quantum-dot-based next-generation lasers, and biosensors, rely on our ability to design and fabricate *ordered* small-scale structures [1–5]. In addition, at the nanoscale, thermodynamic, electronic, and optical properties are size dependent, and their values often differ significantly from those of bulk objects [6–8]. The ability to engineer perfectly ordered nanostructures enables the realization of devices with coherent characteristics that can be "tuned" for specific technological applications [1,3–5,9]. Furthermore, ordered nanostructures are an extremely fertile laboratory to test fundamental quantum-mechanical effects. Unfortunately, current—primarily lithographic—techniques used for miniaturization are reaching their limits [10]. Self-assembly—the spontaneous formation of regular arrays—is emerging as one of the most promising avenues for both miniaturization and fabrication. The primary disadvantage associated with self-assembly is its inability to create long-range-ordered structures. In this Rapid Communication, we use an idea based on the fundamental physics of pattern formation to introduce a strategy to consistently obtain long-range-ordered structures.

Consider an experimental or model system that generates monolayer patterns when a spatially uniform layer of atoms is slowly deposited (e.g., [1,3,9]). Typical large-aspect-ratio patterns in such systems are similar to Fig. 1(a), which herein is generated using a paradigmatic model to be described shortly. In the case shown, relevant control parameters are chosen so that hexagonal patterns are stable. As is evident, the pattern displays locally hexagonal domains; however, it contains multiple grains with differing hexagonal orientations. Also manifest are the presence of concomitant grain boundaries, triple junctions, dislocations, and disclinations. It is this lack of long-range order that prevents the widespread use of self-assembly for many technological applications.

We begin by outlining why defective patterns are so ubiquitous [1,3–5,9,11–14] using one of many paradigmatic models of self-assembly [15–23]. These models contain three processes critical for self-assembly: (a) phase separation, which describes the affinity of monolayer atoms to each other; (b) phase coarsening, which quantifies the interfacial energy between occupied and vacant monolayer domains; and (c) phase refining, due to the strain resulting from inhomogeneous surface stress [14]. Note that (a) and (b) promote while (c) inhibits the growth of homogeneous domains. The model system used in this paper is the following Cahn-Hilliard-type equation [24]:

$$\frac{\partial C}{\partial t} = \nabla^2\left[P(C) - 2\nabla^2 C + \frac{Q}{\pi} I_0\right] \qquad (1)$$

for the spatiotemporal dynamics of the (coarse-grained) fractional coverage $C(x,y)$ on the monolayer under spatially uniform deposition of atoms. Here, $P(C)=\ln(C/1-C)+\Omega(1-2C)$ and

$$I_0 = \int\int \frac{(x-\xi_1)\partial C/\partial \xi_1 + (y-\xi_2)\partial C/\partial \xi_2}{[(x-\xi_1)^2+(y-\xi_2)^2]^{3/2}} d\xi_1 d\xi_2$$

is a spatial integral associated with phase refining [14]. The appearance and stability of patterns depend on three control parameters. The first, Q, is the ratio of the width of an interface between occupied and vacant domains and the nearest-neighbor distance. The second, Ω, characterizes the free-energy function through $P(C)$. The third control parameter, C_0, is the mean coverage $\langle C(x,y)\rangle$ of the monolayer, which is conserved in the model. The pattern shown in Fig. 1(a) is the long-time solution of Eq. (1) reached by evolving a uniform but slightly noisy initial state and is in qualitative agreement with experimental patterns [14].

The model we have adopted (i.e., the Suo-Lu model) is not universal and cannot describe all types of self-assembling systems. However, our central strategy is based only on symmetry and symmetry breaking. Typically (but not necessarily always) such features supercede details of the actual physical system or model [29]. For example, bifurcation of the homogeneous solution to a hexagonal array and the orientation of the array near boundaries are common features of most pattern-forming systems (without up-down

*Corresponding author: psharma@uh.edu

†Corresponding author: gemunu@uh.edu

 ©2008 The American Physical Society

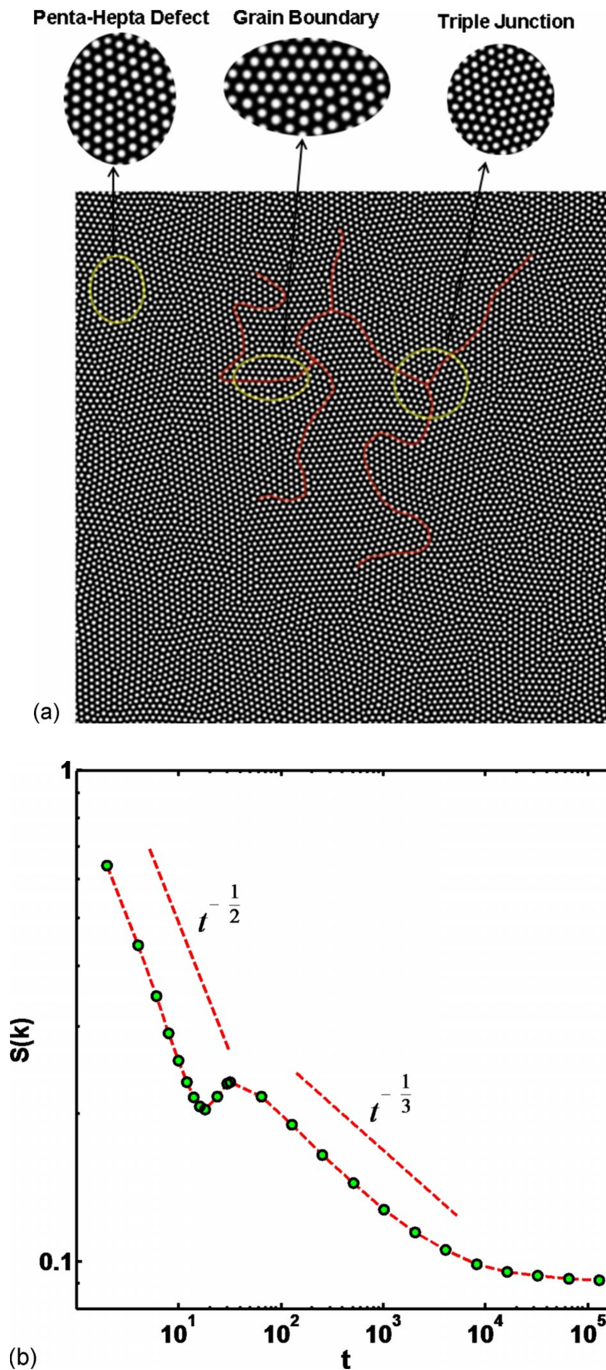

FIG. 1. (Color online) (a) A pattern generated in a two-dimensional domain by integrating model (1) with periodic boundaries and $Q=1.6$ and $\Omega=1.6$. The deposition is given by a random field $C(x,y)=0.38\pm0.01$. Bright dots denote areas of high concentration on the monolayer. Patterns generated using other statistically similar depositions are different in detail, but have similar statistical features. Few representative defects (grain boundaries, triple junctions where two grain boundaries meet, and penta-hepta defects) have been highlighted. (b) The dynamics of the structure factor $S(k)$ during relaxation to pattern (a). Patterns emerge from the uniform background during the first stage when the dynamics is effectively linear. The diffusion length is inversely proportional to $S(k)$ at the end of this stage. The second stage represents domain coarsening. The characteristic domain size in (a) is inversely proportional to the corresponding structure factor.

symmetry) [29]. Thus, conceptually, at least (if not the details), our work is expected to be applicable to many other nonlinear models that govern self-assembling systems not described by the Suo-Lu model. For instance, as elaborated in the discussion, three-dimensional quantum-dot growth (based on interfacial strain) is governed by a different nonlinear model [25,26]; strategies described here are applicable for this case as well.

The model (1) is isotropic and homogeneous, and self-assembly results from spontaneous symmetry breaking as a control parameter (say, C_0) is varied. Symmetry breaking does not lead to a unique solution, but rather to an entire family of equivalent solutions (Goldstone modes or group orbit) [27,28]. In Fig. 1(a), they correspond to arrays with differing hexagonal orientations. In other words, when an isotropic and homogeneous system self-assembles, the hexagonal orientation of a domain can be arbitrary and is determined on the basis of uncontrollable factors like small fluctuations in the deposition. In large-aspect-ratio systems, hexagonal orientations of domains sufficiently far apart are uncorrelated, giving the overall labyrinthine pattern [29–31].

Our goal is to design a system so that the hexagonal orientation in every domain of the pattern is in a predetermined direction. We propose to break the rotational symmetry of the system by using a mask placed a small distance above the substrate to selectively impede deposition. A mask consisting of two arrays of uniform parallel stripes oriented 60° apart [see Fig. 2(a)] can be used to achieve our goal. The directions specified by the mask are two of the six symmetry axes of the hexagonal array that forms on the monolayer.

Geometrical properties of the mask are related to statistical features of a self-assembled labyrinthine structure. First, in order for the pattern to cover the entire domain, it is necessary for the atoms to diffuse to sites covered by the mask. As discussed below, this implies that the width of each stripe is limited by the "diffusion length" [29,32]. The remaining feature defining the mask is the interstripe distance. What is needed is that each region defined by the mask not contain more than a single hexagonal domain; i.e., openings of the mask should be smaller than the characteristic domain size [see Fig. 1(a)]. Once the hexagonal orientation in each domain is fixed, only the translational degeneracy remains as a possible source of pattern irregularity. However, it is known that these "phase defects" are typically removed during pattern relaxation [29,33].

Figure 1(a) is a long-time solution of Eq. (1) with $Q=1.6$ and $\Omega=1.6$. The mean concentration C_0 (=0.38) is chosen to be within the range of stability [0.30, 0.47] of hexagonal arrays. The nearest-neighbor distance can be shown to be $8\pi/Q\sqrt{3}=9.1$ units [34]. The numerical integration of model (1) is conducted for a time of 10^5 (arbitrary) time units using a semi-implicit spectral method [35]. We verify that $C(x,y)$ remains unchanged during the last quarter of this time interval.

There is one subtlety regarding the choice of the domain of integration. Its horizontal extent is 1024 units (lattice size=1) with periodic boundary conditions. However, the oblique set of stripes of the mask will, typically, not match periodically at the top and bottom boundaries. Consequently, the pattern develops defects near these edges. We circumvent

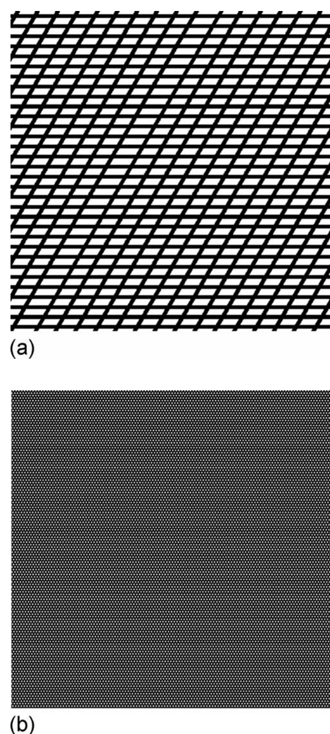

FIG. 2. Results from the numerical integrations of model (1) with masked deposition. The control parameters used in the integration are $Q=1.6$, $\Omega=1.6$, and $C_0=0.38$. (a) The mask used for the integration. The width of stripes on the mask is 8 units. The interstripe distance of the horizontal array is 32 units; the domain shown has an extent of 1024×1024 units. (b) A texture generated by integrating the model in the presence of the mask. Note that the domain of integration is larger and there are defects near the top and bottom edges because the oblique set of stripes of the mask does not match periodically. The image shown is one of height 1024 units away from these edges. The aspect ratio for this pattern is 115.

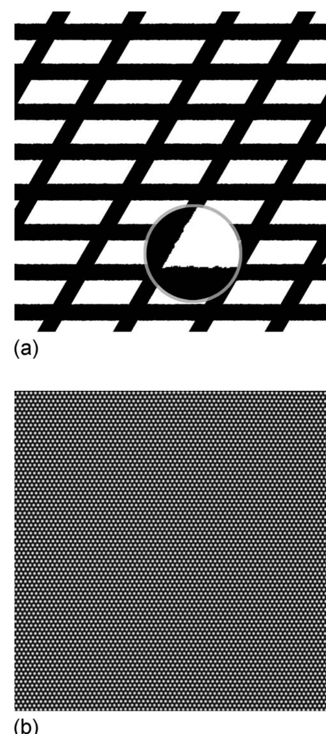

FIG. 3. Hexagonal states generated at $Q=1.0$, $\Omega=1.76$, and $C_0=0.476$ when the mask is irregular. (a) Stripes of the mask are 32 units wide and they are 128 units apart. A stochastic component whose magnitude is up to 8% of the stripe width is added to each site of the edge. (b) The pattern generated continues to be a perfect hexagonal domain. Note that the nearest-neighbor distance is 14.5 units and the horizontal aspect ratio is 72.

this problem by integrating model (1) with a vertical extent of 1280 units and only considering monolayer sites sufficiently far from the top and bottom edges.

Interestingly, the diffusion length and characteristic domain size needed to construct the mask can be estimated using the dynamics of the structure factor $S(k)$ (i.e., the width of the radial projection of the power spectrum), shown in Fig. 1(b) [33,36]. It is known that pattern relaxation occurs in two stages [36,37]. The first, domain growth, is characterized by a $t^{-1/2}$ decay of $S(k)$. During this stage, patterns emerge out of the uniform background. The second stage, domain coarsening, exhibits a significantly slower decay of $S(k)$. The diffusion length and the characteristic long-time domain size are inversely proportional to the values of $S(k)$ at the end of the first stage and at long times, respectively [37]. The mask used for the integration is shown in Fig. 2(a). It consists of two arrays of uniform, equally spaced stripes. The width of each strip is 8 units, smaller than the diffusion length of $\sim$25 units. Neighboring strips are 32 units apart, smaller than the characteristic domain size of $\sim$75 units.

The slow epitaxial deposition was modeled as follows. We initially deposited the monolayer with a coverage $C(x,y)=0.30$ without a mask. The homogeneous solution is the unique stable state here. [Formation of the perfect array is independent of the value of $C(x,y)$ at this point.] Next, the mask is placed above the substrate and the remaining atoms are deposited (with a stochastic term of amplitude 0.01) so that the overall mean concentration is $C_0=0.38$. Now, the stable solution is the broken-symmetry hexagonal state. Patterns similar to Fig. 1(a) are observed in the absence of the mask. In contrast, with the mask in place, the final solution reduces to a perfect hexagonal array, such as the one shown in Fig. 2(b).

We have verified that the orientation of the lattice on which the integration is carried out plays no role in generating ordered patterns. Specifically, if the mask is rotated by 45°, then the perfect hexagonal array obtained is oriented 45° as well. However, it should be noted that the domain used for the integration needs to be extended in both the x and y directions due to the mismatch of the mask. The formation of defects near the boundaries is only an artifact of the numerical algorithm and has no bearing on an experimental setup.

From an experimental perspective, it may be necessary for the mask to consist of wider stripes. This can be implemented by choosing appropriate control parameters. For example, the characteristic domain size at $Q=1.0$, $\Omega=1.76$, and $C_0=0.476$ is larger than that for the previous set of control parameters. Hence, it becomes possible to use a mask with wider stripes and a larger interstripe distance [see Fig. 3(a)]—the nearest-neighbor distance at these control param-

eters is 14.5. The mask has an added feature. Figure 2(a) has a perfect geometric shape; the stripes have fixed width, and the interstripe distance is constant. Currently, it is not possible to create such ideal nanoscale structures. The state-of-the-art lithographic techniques can create stripes to within 5%–10% level of irregularity in the edges [38]. In order to test if masking will prove useful in a more realistic, experimentally relevant setting, we have introduced irregularities by shifting each site of the edge by a random variable whose magnitude is 8% of the mean stripe width. As seen from Fig. 3(b), the formation of an ordered hexagonal pattern is not affected.

The geometrical characteristics of the mask can be deduced from the dynamics of the structure factor. Since nanostripes of width as small as ~20 nm can be produced with current technology, it should be possible to find many experimental systems where perfect monolayer arrays can be engineered. Note that the construction of nanostripes requires very elaborate and time-consuming techniques [39–43]. However, the mask is only used to guide the nanoscale growth and can be reused.

Our studies were conducted on a phenomenological model of epitaxial deposition that is isotropic. Such systems have the largest freedom in the choice of hexagonal orientations following symmetry breaking. Consequently, they are the class of systems where it is most difficult to generate ordered arrays. A logical question now is, what happens with anisotropic systems? For example, single-crystal substrates (typically used) are elastically anisotropic and intrinsically break rotational symmetry. However, a key point to realize is that breaking of the rotational symmetry by itself is insufficient. In fact, masks with single striped arrays also break the isotropy of the system. We have indeed verified that such a mask configuration cannot generate perfect patterns. Two additional ingredients are essential: (i) a striped array in the mask in the second direction, which is exactly oriented 60° to the first array, and (ii) the openings provided by the masks should be smaller than the characteristic domain size.

As alluded to earlier, our general approach involving masking has ramifications beyond the specific illustrative model considered here. For instance, our preliminary work on a model of quantum dot growth with wetting governed by a different nonlinear differential equation [25,26] shows that perfectly ordered arrays can be formed using methods outlined here [44].

This work was partially funded by the National Science Foundation through Grants No. DMS-0607345 (G.H.G.) and No. CMMI-0709293 (G.H.G), the Office of Naval Research through Grant No. N000140510662 (P.S.), the Welch Foundation through Grant No. E-0608 (D.J.K), and grants from the Texas Center for Superconductivity at the University of Houston (G.H.G. and P.S.).

[1] K. Kern *et al.*, Phys. Rev. Lett. **67**, 855 (1991).
[2] J. Z. Zhang *et al.*, *Self-Assembled Nanostructures* (Kluwer Academic/Plenum, New York, 2003).
[3] K. Pohl *et al.*, Nature (London) **397**, 238 (1999).
[4] K. Umezawa *et al.*, Phys. Rev. B **63**, 035402 (2000).
[5] J. E. Guyer and P. W. Voorhees, J. Cryst. Growth **187**, 150 (1998).
[6] V. L. Colvin *et al.*, J. Am. Chem. Soc. **114**, 5221 (1992).
[7] D. Duonghong *et al.*,J. Am. Chem. Soc. **104**, 2977 (1982).
[8] J. Z. Zhang *et al.*, J. Phys. Chem. **98**, 3859 (1994).
[9] R. Plass *et al.*, Nature (London) **412**, 875 (2001).
[10] Y. Chen and A. Pepin, Electrophoresis **22**, 187 (2001).
[11] E. Wahlström *et al.*, Phys. Rev. B **60**, 10699 (1999).
[12] K.-O. Ng and D. Vanderbilt, Phys. Rev. B **52**, 2177 (1995).
[13] F. Glas, Phys. Rev. B **55**, 11277 (1997).
[14] Z. Suo and W. Lu, J. Nanopart. Res. **2**, 353 (2000).
[15] B. G. Orr *et al.*, Europhys. Lett. **19**, 33 (1992).
[16] A. W. Hunt *et al.*, Europhys. Lett. **27**, 611 (1994).
[17] J. E. Guyer and P. W. Voorhees, Phys. Rev. Lett. **74**, 4031 (1995).
[18] V. A. Shchukin *et al.*, Phys. Rev. Lett. **75**, 2968 (1995).
[19] V. A. Shchukin *et al.*, Surf. Sci. **352**, 117 (1996).
[20] I. Daruka and A.-L. Barabasi, Phys. Rev. Lett. **79**, 3708 (1997).
[21] B. J. Spencer and J. Tersoff, Phys. Rev. Lett. **79**, 4858 (1997).
[22] B. J. Spencer *et al.*, Phys. Rev. Lett. **84**, 2449 (2000).
[23] M. Blanariu and B. J. Spencer, IMA J. Appl. Math. **72**, 9 (2007).
[24] J. W. Cahn and J. E. Hilliard, J. Chem. Phys. **28**, 258 (1958).
[25] B. J. Spencer *et al.*, J. Appl. Phys. **73**, 4955 (1993).
[26] A. A. Golovin *et al.*, Phys. Rev. E **68**, 056203 (2003).
[27] M. Field, Trans. Am. Math. Soc. **259**, 185 (1980).
[28] M. Golubitsky and D. S. Schaeffer, *Singularities and Groups in Bifurcation Theory* (Springer-Verlag, New York, 1984).
[29] M. C. Cross and P. C. Hohenberg, Rev. Mod. Phys. **65**, 851 (1993).
[30] M. C. Cross and A. C. Newell, Physica D **10**, 299 (1984).
[31] G. H. Gunaratne *et al.*, Phys. Rev. E **50**, 2802 (1994).
[32] Q. Ouyang and H. L. Swinney, Nature (London) **352**, 610 (1991).
[33] K. R. Elder *et al.*, Phys. Rev. A **46**, 7618 (1992).
[34] S. Hu *et al.*, J. Mech. Phys. Solids **55**, 1357 (2007).
[35] W. Lu and Z. Suo, J. Mech. Phys. Solids **49**, 1937 (2001).
[36] H. R. Schober *et al.*, Phys. Rev. A **33**, 567 (1986).
[37] S. Hu *et al.*, Nonlinearity **17**, 1535 (2004).
[38] *Handbook of Nanotechnology*, edited by B. Bushan (Springer, Berlin, 2003), p. 170.
[39] P. Rai-Choudhary, *Handbook of Microlithography* (SPIE, Bellingham, 1997).
[40] L. Ming *et al.* (unpublished).
[41] R. D. Piner *et al.*, Science **283**, 661 (1999).
[42] S. D. Golladay *et al.*, J. Vac. Sci. Technol. B **18**, 3072 (2000).
[43] J. A. Liddle *et al.*, Microlithogr. World **6**,15 (1997).
[44] F. Shi *et al.* (unpublished).